Vol 18 No 11, November 2009
1674-1056/2009/18(11)/4912-07

Chinese Physics B

© 2009 Chin. Phys. Soc.
and IOP Publishing Ltd

Analytical modelling of end thermal coupling in a solid-state laser longitudinally bonded by a vertical-cavity top-emitting laser diode

Wu Jian(吴 坚)[a)] and H. D. Summers[b)]

[a)] *School of Physics, Beijing University of Aeronautics and Astronautics, Beijing* 100191, *China*
[b)] *School of Physics and Astronomy, Cardiff University, Cardiff CF*24 3*YB, Wales, UK*

(Received 9 February 2009; revised manuscript received 22 March 2009)

The intrinsic features involving a circularly symmetric beam profile with low divergence, planar geometry as well as the increasingly enhanced power of vertical-cavity surface-emitting lasers (VCSELs) have made the VCSEL a promising pump source in direct end bonding to a solid-state laser medium to form the minimized, on-wafer integrated laser system. This scheme will generate a surface contact pump configuration and thus additional end thermal coupling to the laser medium through the joint interface of both materials, apart from pump beam heating. This paper analytically models temperature distributions in both VCSEL and the laser medium from the end thermal coupling regarding surface contact pump configuration using a top-emitting VCSEL as the pump source for the first time. The analytical solutions are derived by introducing relative temperature and mean temperature expressions. The results show that the end contact heating by the VCSEL could lead to considerable temperature variations associated with thermal phase shift and thermal lensing in the laser medium. However, if the central temperature of the interface is increased by less than 20 K, the end contact heating does not have a significant thermal influence on the laser medium. In this case, the thermal effect should be dominated by pump beam heating. This work provides useful analytical results for further analysis of hybrid thermal effects on those lasers pumped by a direct VCSEL bond.

Keywords: solid-state laser, end pump, thermal coupling, vertical-cavity surface-emitting laser
PACC: 4260, 4430

1. Introduction

In general, diode pumped solid-state lasers (DPSS) require focal and beam correcting optics to provide a highly efficient, circular pump beam. This increases the complexity and cost of a laser system as well as the difficulty in making a highly integrated, compact laser device. Recent developments in high power vertical-cavity surface-emitting laser diodes (VCSELs)[1−6] have successfully made the VCSEL an alternative pump source for lasers.[7−10] The advantages of the VCSEL as a pump source lie in its circularly symmetric beam profile with low divergence, planar geometry and easy fabrication in 2-dimensional arrays, which make it possible to develop a direct end contact pump to the laser medium to form a minimized, on-wafer laser device with structural simplification and reduced cost without reduction of pump efficiency. This scheme was first proposed and tested experimentally in Ref.[7], in which the VCSEL was placed in extreme proximity to a solid-state laser crystal and laser output with fundamental mode was obtained.

The monolithic integration of the laser medium with a VCSEL by direct bonding to each other will lead to different thermal effects from those in an ordinary DPSS device, as an additional end contact heating or end thermal coupling to the laser medium occurs through the joint interface of both materials, apart from conventional pump beam heating. This also causes different temperature distribution in the VCSEL due to changed boundary conditions. In this case, the heat flux spreads into the laser medium through the joint interface directly from the VCSEL. So far, all studies on thermal properties of VCSELs and solid-state lasers have been based on single devices or arrays with the surface exposed to the air for the VCSELs[11−15] and an ordinary pump beam heating configuration for DPSS,[16−20] respectively. The results from these studies are not suitable for VCSEL bonded solid-state lasers due to the different thermal boundary conditions and heating mechanism. No papers have presented modelling and analysis of the temperature characteristics and thermal effects of VCSEL pumped solid-state lasers with the longitudinal bond

scheme.

Therefore, it is important to analyse and assess the thermal effects on the laser system from end thermal coupling or end contact heating in order to develop VCSEL bonded solid-state lasers. Although the thermal effect from pump beam heating still plays a role in the VCSEL bonded laser medium, it has been investigated well for ordinary DPSS devices and thus is not what we are concerned about here. In this paper, the temperature distributions in the laser medium and the VCSEL due to the end contact heating in the VCSEL bonded solid-state laser are modelled analytically for the first time to our knowledge. Analytical solutions characterizing temperature distributions in both materials relating to the contact heating are obtained successfully, and provide an useful tool not only for further analysis of thermal effects in VCSEL bonded solid-state lasers, but also for analysing other VCSEL bonded devices.[21]

2. Calculation model

When the solid-state laser medium is bonded longitudinally by the VCSEL, a contact pump configuration is formed and thus end thermal coupling occurs. In this case, the heat flux from the VCSEL spreads into the laser medium through the joint interface of both materials by conduction and leads to variation of the temperature distribution on the VCSEL surface as well as an additional temperature field in the laser medium, in comparison with a non-touch pump configuration. To analyse and characterize the temperature characteristics in the VCSEL and the laser medium caused by end contact heating, an analytical thermal model is created and shown in Fig.1, in which pump beam heating is excluded.

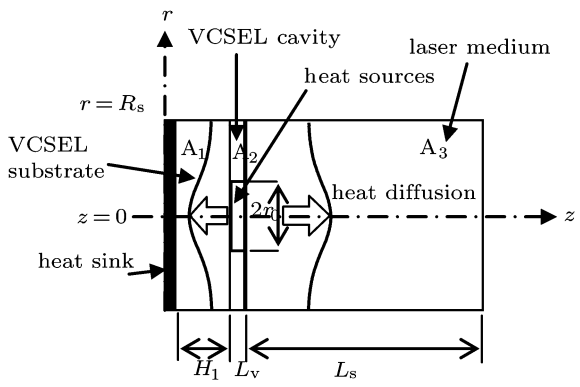


Fig.1. Diagram of end contact heating in a solid-state laser bonded by a VCSEL.

The VCSEL chip is regarded as a disc with all heat sources concentrated in the region, $r \leq r_0$, which corresponds to the current injection area and within the VCSEL cavity. The thermal model of the VCSEL is similar to that described in Ref.[11], but with a different boundary condition for the top-surface. The heating regions of the model in Fig.1 can be divided into three sections which correspond to VCSEL substrate A_1, VCSEL cavity A_2 and laser medium A_3 with lengths H_1, L_v and L_s, respectively. The heat generated by heat sources in the cavity region of the VCSEL diffuses to both the substrate A_1 and the laser medium A_3 and satisfies the following boundary conditions.

All sides of the model and bottom of the VCSEL are assumed to have a fixed temperature, for example, ambient temperature, which can be realized by heat sink control in experiment. The light output end of the laser medium can be processed approximately as a heat-isolated surface.[16] Thus, the boundary conditions based on the above consideration can be written mathematically as

$$z = 0, \quad T_1 = 0, \tag{1}$$

$$r = R_s, \quad T_{1,2,3} = 0, \tag{2}$$

$$z = H_1 + L_v + L_s, \quad \frac{\partial T_3}{\partial z} = 0, \tag{3}$$

where T_1, T_2 and T_3 represent the relative temperatures of three sections A_1, A_2 and A_3 to the ambient temperature, respectively. The temperature continuity at the interfaces $r = r_0$, $z = H_1$ and $z = H_1 + L_v$ allows additional conditions given by

$$r = r_0, \quad T' = T'', \tag{4}$$

$$r = r_0, \quad \frac{\partial T'}{\partial r} = \frac{\partial T''}{\partial r}, \tag{5}$$

$$z = H_1, \quad T_1 = T_2, \tag{6}$$

$$z = H_1, \quad \frac{\partial T_1}{\partial z} = \frac{\partial T_2}{\partial z}, \tag{7}$$

$$z = H_1 + L_v, \quad T_2 = T_3, \tag{8}$$

$$z = H_1 + L_v, \quad \frac{\partial T_2}{\partial z} = \frac{\partial T_3}{\partial z}, \tag{9}$$

where T' and T'' are the relative temperatures of the regions $r \leq r_0$ and $r > r_0$ to the ambient temperature, respectively.

3. Analytical solutions

A general steady-state heat conduction equation for the model in Fig.1 can be written as

$$\frac{1}{r}\frac{\partial}{\partial r}\left(r\frac{\partial T}{\partial r}\right)+\frac{\partial^2 T}{\partial z^2}=-\frac{\dot{q}}{\kappa}, \tag{10}$$

where $\dot{q}$ is the rate of total thermal energy generated per unit volume from all heat sources in the VCSEL. κ is thermal conductivity, whose value is related to the materials. The general solution of Eq.(10) for each section of the model can be obtained by the following calculations.

Section A_1 of the model is the VCSEL substrate. Thus, there is no heat source in there and the boundary conditions of Eqs.(1) and (2) are satisfied. The right side of Eq.(10) goes to zero and the general solution can be obtained as

$$T_1(r,z)=\sum_{n=1}^{\infty}\left[B_n\sinh(\lambda_n z)\right]\mathrm{J}_0(\lambda_n r), \tag{11}$$

where λ_n is a specific series of coefficients satisfying the boundary condition of Eq.(2), i.e. $\mathrm{J}_0(\lambda_n R_\mathrm{s})=0$, B_n is a series of constants, $\mathrm{J}_0(\lambda_n r)$ is the zero-order Bessel function.

Section A_2 involves all heat sources concentrated in the region $r\le r_0$ in the VCSEL. Thus, the thermal conduction equation for the section A_2 is written as

$$\frac{1}{r}\frac{\partial}{\partial r}\left(r\frac{\partial T_2}{\partial r}\right)+\frac{\partial^2 T_2}{\partial z^2}=\begin{cases}-\dfrac{\dot{q}}{\kappa}, & 0<r\le r_0,\\ 0, & r_0<r\le R_\mathrm{s}.\end{cases} \tag{12}$$

Since section A_2, i.e. the VCSEL cavity, is generally very short, which is typically about 10 μm in length, there is little difference in temperature over the whole cavity length under the condition of steady-state heat flux distribution. Thus, a mean temperature over section A_2 along the z-axis can be introduced as a measure of central temperature from the heat sources of the VCSEL, which can be written as

$$\langle T_2(r)\rangle=\frac{1}{L_\mathrm{v}}\int_{H_1}^{H_1+L_\mathrm{v}}T_2(r,z)\,\mathrm{d}z. \tag{13}$$

This brings additional boundary conditions at the interfaces between the sections A_1, A_2 and A_3, which are given by

$$T_1(r,H_1)\approx\langle T_2(r)\rangle\approx T_3(r,L_1), \tag{14}$$

where $L_1=H_1+L_\mathrm{v}$. Thus, the integral over the section A_2 can be executed on both sides of Eq.(12), which yields

$$\frac{1}{r}\frac{\partial}{\partial r}\left(r\frac{\partial\langle T_2(r)\rangle}{\partial r}\right)+\frac{1}{L_\mathrm{v}}\left(\left.\frac{\partial T_2}{\partial z}\right|z=H_1+L_\mathrm{v}-\left.\frac{\partial T_2}{\partial z}\right|z=H_1\right)=\begin{cases}-\dfrac{\dot{q}}{\kappa}, & 0<r\le r_0,\\ 0, & r_0<r\le R_\mathrm{s}.\end{cases} \tag{15}$$

Since there is no heat source within section A_3 either, the right side of Eq.(10) equals zero. Under the boundary conditions of Eqs.(2) and (3), the general solution of the conduction equation for section A_3 can be obtained as

$$T_3(r,z)=\sum_{n=1}^{\infty}C_n[\cosh(\lambda_n z)-\tanh(\lambda_n L_\mathrm{tot})\cdot\sinh(\lambda_n z)]\cdot\mathrm{J}_0(\lambda_n r), \tag{16}$$

where $L_\mathrm{tot}=H_1+L_\mathrm{v}+L_\mathrm{s}$ is the total length of the VCSEL and laser medium, C_n is a series of constants. Thus, the differential temperatures at $z=H_1$ of section A_1 and $z=H_1+L_\mathrm{v}$ of section A_3 can be obtained from Eqs.(11) and (16), respectively, and are given by

$$\left.\frac{\partial T_1(r,z)}{\partial z}\right|_{z=H_1}=\sum_{n=1}^{\infty}B'_n\lambda_n\mathrm{J}_0(\lambda_n r), \tag{17}$$

$$\left.\frac{\partial T_3(r,z)}{\partial z}\right|_{z=L_1}=\sum_{n=1}^{\infty}C'_n\lambda_n\mathrm{J}_0(\lambda_n r), \tag{18}$$

where $B'_n=B_n\cosh(\lambda_n H_1)$ and

$$C'_n=\sinh(\lambda_n L_1)-\tanh(\lambda_n L_\mathrm{tot})\cdot\cosh(\lambda_n L_1).$$

Thus, substituting Eqs.(17) and (18) as well as the temperature continuity conditions of Eqs.(7) and (9) into Eq.(15) yields

$$\frac{1}{r}\frac{\partial}{\partial r}\left(r\frac{\partial\langle T_2(r)\rangle}{\partial r}\right)+\frac{1}{L_{\mathrm{v}}}\left[\sum_{n=1}^{\infty}\left(C_n'-B_n'\right)\lambda_n \mathrm{J}_0(\lambda_n r)\right]=\begin{cases}-\dfrac{\dot{q}}{\kappa}, & 0<r\le r_0\\ 0, & r_0<r\le R_{\mathrm{s}}.\end{cases} \tag{19}$$

Integrating each item of Eq.(19) in the radial direction and applying the temperature continuity conditions of Eqs.(4) and (5) at the interface $r=r_0$ as well as the following conditions to the integral of Eq.(19),

$$r=R_{\mathrm{s}},\quad \langle T_2\rangle=0, \tag{20}$$

$$r=0,\quad \frac{\partial\langle T_2\rangle}{\partial r}=0, \tag{21}$$

we can obtain the temperature, $\langle T_2(r)\rangle$,

$$\langle T_2(r)\rangle=\frac{1}{L_{\mathrm{v}}}\left[\sum_{n=1}^{\infty}\frac{\left(C_n'-B_n'\right)}{\lambda_n}\mathrm{J}_0(\lambda_n r)\right]+f(r), \tag{22}$$

where

$$f(r)=\frac{\dot{q}r_0^2}{4\kappa}\begin{cases}-2\ln\dfrac{r_0}{R_{\mathrm{s}}}+1-\left(\dfrac{r}{r_0}\right)^2, & 0<r\le r_0,\\ -2\ln\dfrac{r}{R_{\mathrm{s}}}, & r_0<r\le R_{\mathrm{s}}.\end{cases} \tag{23}$$

The constants B_n, C_n and $C_n'-B_n'$ are obtained by substituting Eqs.(11) and (16) into the condition Eq.(14), which are

$$C_n=D_nB_n, \tag{24}$$

$$C_n'-B_n'=G_nB_n, \tag{25}$$

$$D_n=\frac{\sinh(\lambda_nH_1)\cosh(\lambda_nL_{\mathrm{tot}})}{\cosh(\lambda_nL_{\mathrm{s}})}, \tag{26}$$

$$G_n=-\frac{\cosh\left[\lambda_n\left(L_{\mathrm{s}}+H_1\right)\right]}{\cosh(\lambda_nL_{\mathrm{s}})}. \tag{27}$$

Therefore, the temperature $\langle T_2(r)\rangle$ can be expressed as

$$\langle T_2(r)\rangle=\frac{1}{L_{\mathrm{v}}}\left[\sum_{n=1}^{\infty}\frac{G_nB_n}{\lambda_n}\mathrm{J}_0(\lambda_nr)\right]+f(r). \tag{28}$$

The function $f(r)$ is characterized by substituting Eqs.(11) and (28) into Eq.(14), which is

$$\sum_{n=1}^{\infty}H_n\mathrm{J}_0(\lambda_nr)=f(r), \tag{29}$$

where

$$H_n=B_n\left[\sinh(\lambda_nH_1)-G_n/L_{\mathrm{v}}\lambda_n\right]. \tag{30}$$

Using Bessel function theory, we can write the constant H_n in Eq.(30) as

$$H_n=\frac{\int_0^{R_{\mathrm{s}}}rf(r)\,\mathrm{J}_0(\lambda_nr)\,\mathrm{d}r}{\int_0^{R_{\mathrm{s}}}r\mathrm{J}_0^2(\lambda_nr)\,\mathrm{d}r}. \tag{31}$$

Thus, the constant H_n is obtained by substituting Eq.(24) into Eq.(31), which is

$$H_n=\frac{2\dot{q}r_0}{\kappa R_{\mathrm{s}}^2}\cdot\frac{\mathrm{J}_1(\lambda_nr_0)}{\lambda_n^3\cdot\mathrm{J}_1^2(\lambda_nR_{\mathrm{s}})}. \tag{32}$$

The constant B_n is obtained by substituting Eq.(32) into Eq.(30), which is

$$B_n=\frac{2\dot{q}r_0L_{\mathrm{v}}}{\kappa R_{\mathrm{s}}^2}\cdot\frac{1}{\lambda_n^2}\cdot\frac{1}{L_{\mathrm{v}}\lambda_n\sinh(\lambda_nH_1)-G_n}\cdot\frac{\mathrm{J}_1(\lambda_nr_0)}{\mathrm{J}_1^2(\lambda_nR_{\mathrm{s}})}. \tag{33}$$

The constants C_n, $C_n'-B_n'$ are obtained by substituting Eq.(33) into Eqs.(24) and (25). Finally, the analytical solutions characterizing the temperature distributions of the VCSEL top-surface and the laser medium due to the end contact heating are obtained as

$$\langle T_2(r)\rangle=\frac{2\dot{q}r_0L_{\mathrm{v}}}{\kappa R_{\mathrm{s}}^2}\sum_{n=1}^{\infty}\frac{1}{\lambda_n^2}\cdot\frac{\sinh(\lambda_nH_1)}{L_{\mathrm{v}}\lambda_n\sinh(\lambda_nH_1)-G_n}\cdot\frac{\mathrm{J}_1(\lambda_nr_0)}{\mathrm{J}_1^2(\lambda_nR_{\mathrm{s}})}\cdot\mathrm{J}_0(\lambda_nr), \tag{34}$$

$$T_3(r,z)=\frac{2\dot{q}r_0L_{\mathrm{v}}}{\kappa R_{\mathrm{s}}^2}\sum_{n=1}^{\infty}\frac{D_n}{\lambda_n^2}\cdot\frac{\cosh\left[\lambda_n\left(L_{\mathrm{tot}}-z\right)\right]}{\left[\cosh(\lambda_nL_{\mathrm{tot}})\cdot\left[L_{\mathrm{v}}\lambda_n\sinh(\lambda_nH_1)-G_n\right]\right.}\cdot\frac{\mathrm{J}_1(\lambda_nr_0)}{\mathrm{J}_1^2(\lambda_nR_{\mathrm{s}})}\cdot\mathrm{J}_0(\lambda_nr), \tag{35}$$

where G_n is determined by Eq.(27).

In general, it is difficult to derive the values of total thermal energy generation rate $\dot{q}$ and thermal conductivity κ exactly from the known conditions in order to describe the absolute temperatures given by Eqs.(34) and (35). However, this problem can be removed by introducing a relative temperature to the central temperature at $r = 0$. Using this treatment, we can rewrite Eq.(35) as

$$T_3^*(r,z) = \frac{T_3(r,z)}{T_3(0, H_1 + L_{\rm v})}. \tag{36}$$

Thus, the actual temperature variation within the laser medium due to end contact heating can be characterized by taking the product of the relative temperature $T_3^*(r,z)$ determined by Eq.(36) and the central temperature $T_{\rm vc} = T_3(0, H_1 + L_{\rm v})$, which represents the temperature of VCSEL heat sources and can be measured by experiment

$$T_3(r,z) = T_{\rm vc} \cdot T_3^*(r,z). \tag{37}$$

Based on Eq.(37), a 3-dimensional temperature distribution in the laser medium from end thermal coupling is plotted in Fig.2. The VCSEL is 100 μm in diameter with cavity length of 10 μm and substrate thickness of 150 μm. The laser medium may be a solid-state crystal or other laser material with an optical aperture of 2.0 mm in diameter and a medium length of 500 μm. The central temperature of the VCSEL is changed by $\Delta T_{\rm vc} = 100$ K. Obviously, the end thermal coupling from the VCSEL produces abrupt temperature variations, i.e. high differential temperatures, in both radial and axial directions in the laser medium. The high differential temperatures in both directions mean that the end contact heating from the VCSEL may lead to considerable thermal phase shift and thus thermal lensing in the laser medium, apart from the thermal guiding effects induced by the pump beam heating.

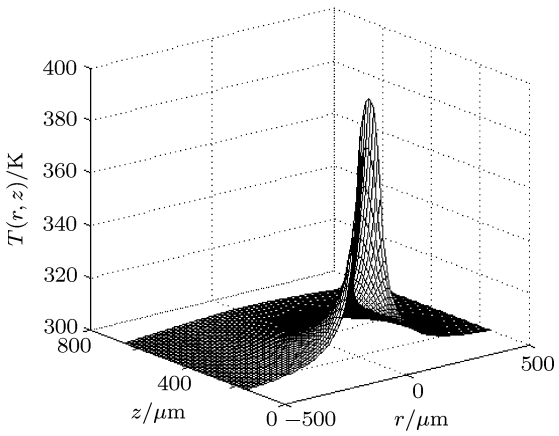


Fig.2. The 3-dimensional temperature distribution within the laser medium from end thermal coupling with a VCSEL pump source.

To investigate the total thermal phase shift caused by the end contact heating in the laser medium, the mean temperature over the laser medium length is taken by integration of Eq.(35) along the z-axis, which results in

$$\langle T_3(r)\rangle = \frac{2\dot{q} r_0 L_{\rm v}}{\kappa_a(x) R_{\rm s}^2 L_{\rm s}} \sum_{n=1}^{\infty} P_n \cdot \frac{\mathrm{J}_1(\lambda_n r_0)}{\mathrm{J}_1^2(\lambda_n R_{\rm s})} \cdot \mathrm{J}_0(\lambda_n r), \tag{38}$$

where

$$P_n = \frac{1}{\lambda_n^3} \cdot \frac{\sinh(\lambda_n H_1) \cdot \sinh(\lambda_n L_{\rm s})}{L_{\rm v}\lambda_n \sinh(\lambda_n H_1)\cosh(\lambda_n L_{\rm s}) + \cosh[\lambda_n (L_{\rm s} + H_1)]}. \tag{39}$$

Applying a similar treatment to Eq.(35), we can express Eq.(38) by using a relative temperature as well, which is given by

$$\langle T_3(r)\rangle = T_{\rm vc} \cdot \frac{\langle T_3(r)\rangle}{T_3(0, H_1 + L_{\rm v})}. \tag{40}$$

Thus, the temperature variation $\langle \Delta T_3(r)\rangle$ relative to the room temperature, 300 K, with increasing central temperatures of the VCSEL is plotted in Fig.3.

The data in Figs.2 and 3 show that there are considerable temperature variations in both radial and axial directions within the laser medium when the joint interface of both materials is heated up by the

VCSEL. Particularly, the high differential temperatures make sense in causing thermal phase change and thus the thermal lensing effect due to the generation of a large thermal index gradient. When the central temperature increase of the VCSEL is less than 20 K, the end contact heating does not make a significant thermal phase change in the laser medium, as the central mean temperature along the z-axis changes around by one degree. In this case, the thermal effect should be dominated by pump beam heating. This modelling provides useful analytical solutions for further analysing hybrid thermal effects in VCSEL bonded solid-state lasers.

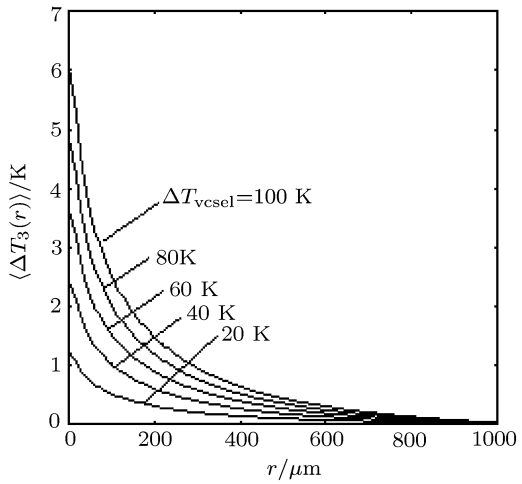


Fig.3. Mean temperature over laser medium length as a function of radius with different central temperatures of the VCSEL.

4. Conclusion

The development of high power VCSELs and the intrinsic VCSEL features of a circularly symmetric beam profile with low divergence and planar geometry have made the VCSEL a promising device as a direct pump source for solid-state lasers by longitudinally bonding to the laser medium to form a minimized, on-wafer laser device. This scheme generates a direct contact pump configuration and thus additional end thermal coupling to the laser medium through the joint interface of both materials in comparison with the pump configuration of an ordinary DPSS device. To investigate and characterize the thermal influences from the end thermal coupling, the temperature distributions in the VCSEL and the laser medium from the end contact heating are modelled analytically by using a top-emitting VCSEL as the pump source. Analytical solutions of the heat conduction equation for this case are derived. The temperature distributions in the laser medium and the VCSEL are characterized by introducing relative temperature and mean temperature expressions. The results show that end thermal coupling from the VCSEL can cause abrupt temperature variations in both radial and axial directions in the laser medium. The high differential temperatures in both directions within the laser medium mean that there will be considerable thermal phase changes and thus a thermal lensing effect, caused by the end contact heating of the VCSEL. When the central temperature increase of the VCSEL is less than 20 K, the end contact heating does not make a significant thermal phase change in the laser medium, as the central mean temperature over the laser medium changes around by one degree. In this case, the thermal effect should be dominated by pump beam heating. This modelling provides useful analytical solutions not only for further analysis of hybrid thermal guiding effects in VCSEL bonded solid-state lasers, but also for analysing other VCSEL integrated devices, in which the VCSELs are directly bonded to the chips.

References

[1] Yoshikawa M, Murakami A, Sakurai J, Nakayama H and Nakamura T 2005 *Proceedings of the 55*th *Electronic Components and Technololy Conference* Florida, USA, May 31–June 3, 2005 p1353

[2] Li H Q, Zhang J, Cui D F, Xu Z Y, Ning Y Q, Yan C L, Qin L, Liu Y, Wang L J and Cao J L 2004 *Acta Phys. Sin.* **53** 2986 (in Chinese)

[3] Li T, Ning Y Q, Sun Y F, Qin L, Yan C L, Liu Y and Wang L J 2005 *Proceedings of SPIE: Optoelectronic Materials and Devices for Optical Communications* Shanghai, China, November 7–10, 2005 p602002

[4] Miller M, Grabherr M, Jaeger R, Unold H J and Ebeling K J 2000 *Conference Digest-IEEE 17th International Semiconductor Laser Conference* California, USA, September 25–28, 2000 p63

[5] Michalzik R, Grabherr M, Jager R, Miller M and Ebeling K J 1998 *Proceedings of SPIE: Optoelectronic Materials and Devices* Taipei, Taiwan, China July 9–11, 1998 p187

[6] Hofmann W, Gorblich M, Ortsiefer M, Bohm G and Amann M C 2007 *Electron. Lett.* **43** 1025

[7] Wu J, Iordache G, Summers H D and Roberts J S 2001 *Opt. Commun.* **196** 251

[8] Lan Y P, Chen Y F, Huang K F, Lai H C and Pan J S 2002 *Photon. Technol. Lett.* **14** 272

[9] O'Brien J D, Lee P T, Cao J R, Kim C, Kim W J, Choi S J and Dapkus P D 2002 *Conference on Lasers and Electro-Optics* California, USA, May 19–24, 2002 p295

[10] Lee P T, Cao J R, Choi S J, Wei Z J, O'Brien J D and Dapkus P D 2001 *The 14th Annual Meeting of the IEEE Lasers and Electro-Optics Society* San Diego, USA, November 12–13, 2001 p651

[11] Wu J 2006 *Acta Phys. Sin.* **55** 5848 (in Chinese)

[12] Rissons A, Mollier J C, Toffano Z, Destrez A and Pez M M 2003 *SPIE* **4994** 100

[13] Leal A A, Osinski M and Conforti E 1998 *IEEE Trans. of Microwave Theory and Techniques* **46** 208

[14] Hadley G R, Lear K L, Warren M E, Choquette K D, Scott J W and Corzine S W 1996 *IEEE J. Quant. Electron.* **32** 607

[15] Nakwaski W 1996 *Opt. Quant. Electron.* **28** 335

[16] Cousins A K 1992 *IEEE J. Quant. Electron.* **28** 1057

[17] Farrukh U O, Buoncristiani A M and Byvik C E 1988 *IEEE J. Quant. Electron.* **24** 2253

[18] Weber R, Neuenschwander B and Weber H P 1999 *Optical Materials* **11** 245

[19] Usievich B A, Sychugov V A, Pigeon F and Tishchenko A 2001 *IEEE J. Quant. Electron.* **37** 1210

[20] Sabaeian M, Nadgaran H and Mousave L 2008 *Appl. Opt.* **47** 2317

[21] Pu R, Wilmsen C W, Choquette K D and Geib K M 1999 *SPIE* **3805** 87